Advances in Theoretical and Applied Mathematics
ISSN 0973-4554 Volume 14, Number 2 (2019), pp. 89-104

http://www.ripublication.com

Propagation of Plane Waves in a Fiber-Reinforced Thermoelastic Medium under Lord-Shulman Model

Seema Thakran*, Rajesh Kumar*, Ankush Gunghas, Kapil Kumar Kalkal***

**Department of Applied Sciences, School of Engineering and Technology, The NorthCap University, Gurgaon-122017, Haryana, India.*

***Department of Mathematics, Guru Jambheshwar University of Science and Technology, Hisar-125001, Haryana, India*

Abstract

The current manuscript is an attempt to discuss the propagation of plane waves from the free surface of a homogeneous, anisotropic, fiber-reinforced thermoelastic medium under the purview of Lord-Shulman model of generalized thermoelasticity. It has been observed that three coupled plane waves travel through the medium with distinct speeds. Using appropriate boundary conditions, the amplitude and energy ratios of various reflected waves are calculated and the numerical computations have been carried out with the help of MATLAB programming. The numerical values of reflection coefficients are presented graphically to exhibit the effect of fiber-reinforcement. The expressions of energy ratios have also been obtained in explicit form and are shown graphically as functions of angle of incidence. It has been verified that during reflection phenomena, the sum of energy ratios is equal to unity at each angle of incidence.

Keywords: Fiber-Refinforced; Reflection; Lord-Shulman model; Amplitude ratios; Energy ratios.

MSC 2010: 74A15, 80A20.

1. INTRODUCTION

The classical theory of thermoelasticity, involving infinite speed of propagation of thermal signals, contradicts physical facts. To eliminate the paradox of infinite speed for propagation of thermoelastic disturbances, various generalized thermoelasticity models have been developed, which involve hyperbolic governing equations. Among these generalized theories, the extended thermoelasticity theory introduced by Lord

* Corresponding author email: kapilkalkal_gju@rediffmail.com

and Shulman (L-S) [1] involving one relaxation time (known as single-phase-lag model) and the temperature-rate-dependent theory of thermoelasticity proposed by Green and Lindsay [2] involving two relaxation times, are two important models of generalized theory of thermoelasticity. After that, providing sufficient basic modifications in governing equations, Green and Naghdi [3-5] established three different models of thermoelasticity, referred to as G-N theory of types I, II, III. Generalized thermoelasticity theories are more realistic than conventional thermoelasticity theories in dealing with practical problems, such as laser units, energy channels, nuclear reactors etc.

Wave propagation in a reinforced medium plays an important role in civil engineering and geophysics. Fiber reinforced composites are used in a variety of structures due to their low weight and high strength. Belfield *et al*. [6] gave the idea of introducing continuous self-reinforcement at every point of an elastic solid. Chattopadhyay and Choudhury [7] investigated the reflection and transmission of magneto-elastic shear waves in a self-reinforced media. The problem of surface wave propagation in a fiber-reinforced, anisotropic elastic media was explained by Sengupta and Nath [8]. Singh and Singh [9] explained the problem of reflection of plane waves at the free surface of a fiber-reinforced elastic half-space. Singh [10] discussed the propagation of plane waves in a fiber-reinforced, anisotropic, generalized thermoelastic media and derived the frequency equation.

Abbas [11] examined the nature of plane waves in a fiber-reinforced, anisotropic thermoelastic half-space by applying the theory of thermoelasticity with energy dissipation. Gupta and Gupta [12] explored the effect of initial stress on the propagation of plane waves in a rotating, transversely isotropic medium in the context of G-N theory of types II and III. Kumar *et al*. [13] studied the reflection of plane waves at the free surface of thermally conducting micropolar elastic medium with two temperatures. Kumar *et al*. [14] investigated the propagation of Rayleigh surface waves in an isotropic, microstretch, thermo-diffusive solid medium under a layer of inviscid liquid. Ailawalia *et al*. [15] presented a study on two-dimensional deformation of fiber reinforced, micropolar, thermoelastic medium in the context of Green-Lindsay theory. Said and Othman [16] scrutinized the effect of gravity field in a fiber-reinforced thermoelastic medium with temperature dependent properties under three-phase-lag theory of generalized thermoelasticity. Abouelregal [17] solved a two-dimensional problem of generalized thermoelasticity for a fiber-reinforced, anisotropic thick plate under initial stress in the context of fractional order heat conduction theory. Kalkal *et al*. [18] presented a study on the thermo-viscoelastic interactions in a homogeneous, isotropic, micropolar, elastic medium with rotation under three-phase-lag effects. Deswal *et al*. [19] investigated the effects of gravity and initial stress in a fiber-reinforced, anisotropic, thermoelastic half-space with diffusion.

In the present manuscript, we have studied the possibility of wave propagation in a fiber-reinforced, anisotropic thermoelastic medium in the context of L-S model. The formula for amplitude ratios and energy ratios corresponding to various reflected waves have been evaluated, when a set of coupled waves strikes obliquely at boundary surface of the assumed model and their variations with angle of incidence are presented graphically. The phase speeds of various existing waves are computed and their variations are depicted graphically against angle of incidence. It has been verified that during reflection phenomena, the sum of energy ratios is equal to unity at each angle of incidence. Some comparisons have been made in figures to estimate the effects of fiber-reinforcement parameters. The propagation of waves in such materials has many practical applications in various fields such as atomic physics, industrial engineering, aerospace, thermal power plants as well as chemical pipes.

2 BASIC EQUATIONS

The field equations and constitutive relations for a fiber-reinforced linear thermoelastic anisotropic medium with respect to the reinforcement direction $\vec{a}$ in the context of L-S theory are:

Constitutive relations

$$\sigma_{ij} = \lambda e_{kk}\delta_{ij} + 2\mu_T e_{ij} + \alpha\left(a_k a_m e_{km}\delta_{ij} + a_i a_j e_{kk}\right)$$
$$+2\left(\mu_L - \mu_T\right)\left(a_i a_k e_{kj} + a_j a_k e_{ki}\right) + \beta a_k a_m e_{km} a_i a_j - \beta_{ij}\theta\delta_{ij}. \quad (1)$$

Equation of motion

$$\sigma_{ji,j} = \rho\ddot{u}_i. \quad (2)$$

Heat conduction equation

$$K_{ij}\theta_{,ij} = \left(1 + \tau_0\frac{\partial}{\partial t}\right)\left(\rho c_E\dot{\theta} + T_0\beta_{ij}\dot{u}_{i,j}\right). \quad (3)$$

Strain-displacement relation

$$e_{ij} = \frac{1}{2}\left(u_{i,j} + u_{j,i}\right), \quad (4)$$

where σ_{ij}'s are the components of stress, e_{ij}'s are the components of strain, $\alpha, \beta, \left(\mu_L - \mu_T\right)$ are reinforcement parameters, λ, μ_T are elastic constants, δ_{ij} is the Kronecker delta, $\theta = T - T_0$, T is absolute temperature, T_0 is temperature of the medium in its natural state assumed to be $\left|\frac{\theta}{T_0}\right| << 1$, $\vec{a} = \left(a_1, a_2, a_3\right)$, where $a_1^2 + a_2^2 + a_3^2 = 1$, $\vec{a} = \left(1, 0, 0\right)$ is the fiber-direction, ρ is the mass density, β_{ij} is the thermal elastic coupling tensor, c_E is the specific heat at constant strain, K_{ij} is thermal conductivity and τ_0 is the thermal relaxation time.

In the above equations, a comma denotes material derivative and the summation convention is used.

3 FORMULATION OF THE PROBLEM

We consider the problem of a fiber-reinforced anisotropic thermoelastic half-space in the context of L-S theory. Choose a Cartesian co-ordinate system (*x, y, z*) having the surface of the half-space as the plane $x = 0$, with *x*-axis pointing vertically downwards into the medium. We restrict our analysis to *xy*-plane. Thus, all the considered functions will depend on time *t* and the coordinates *x* and *y*. So, the displacement vector $\vec{u}$ will have the components:

$$u = u_x = u(x, y, t),\ v = u_y = v(x, y, t),\ w = u_z = 0. \tag{5}$$

Taking into consideration (1), the requisite stress components are given by

$$\sigma_{xx} = A_{11}\frac{\partial u}{\partial x} + A_{12}\frac{\partial v}{\partial y} - \beta_{11}\theta, \tag{6}$$

$$\sigma_{yy} = A_{12}\frac{\partial u}{\partial x} + A_{13}\frac{\partial v}{\partial y} - \beta_{22}\theta, \tag{7}$$

$$\sigma_{xy} = \mu_L\left(\frac{\partial u}{\partial y} + \frac{\partial v}{\partial x}\right), \tag{8}$$

where

$$A_{11} = \lambda + 2(\alpha + \mu_T) + 4(\mu_L - \mu_T) + \beta,\ A_{12} = \lambda + \alpha,\ A_{13} = \lambda + 2\mu_T.$$

Inserting the stresses defined in eqs. (6)-(8) into (2) along with the consideration of two-dimensional problem, the equation of motion takes the form:

$$\rho\frac{\partial^2 u}{\partial t^2} = A_{11}\frac{\partial^2 u}{\partial x^2} + A_{21}\frac{\partial^2 v}{\partial x\partial y} + \mu_L\frac{\partial^2 u}{\partial y^2} - \beta_{11}\frac{\partial\theta}{\partial x}, \tag{9}$$

$$\rho\frac{\partial^2 v}{\partial t^2} = \mu_L\frac{\partial^2 v}{\partial x^2} + A_{21}\frac{\partial^2 u}{\partial x\partial y} + A_{13}\frac{\partial^2 v}{\partial y^2} - \beta_{22}\frac{\partial\theta}{\partial y}. \tag{10}$$

From (3), one can obtain

$$\left(K_{11}\frac{\partial^2\theta}{\partial x^2} + K_{22}\frac{\partial^2\theta}{\partial y^2}\right) = \left(1 + \tau_0\frac{\partial}{\partial t}\right)\left(\rho c_E\dot{\theta} + T_0\beta_{11}\frac{\partial\dot{u}}{\partial x} + T_0\beta_{22}\frac{\partial\dot{v}}{\partial y}\right), \tag{11}$$

where

$$A_{21} = A_{12} + \mu_L.$$

In order to find non-dimensional forms of the governing equations, let us define the following set of dimensionless variables:

$$(x', y', u', v') = c_0\eta_0(x, y, u, v), (t', \tau_q') = c_0^2\eta_0(t, \tau_q),$$

$$\sigma'_{ij} = \frac{\sigma_{ij}}{\rho c_0^2}, \theta' = \frac{\beta_{11}}{\rho c_0^2}\theta, \tag{12}$$

where

$$\eta_0 = \frac{\rho c_E}{K_{11}}, c_0^2 = \frac{A_{11}}{\rho}.$$

Making use of dimensionless parameters, eqs. (6)-(11) recast into the following forms (dropping the primes):

$$\sigma_{xx} = \frac{\partial u}{\partial x} + B_1 \frac{\partial v}{\partial y} - \theta, \tag{13}$$

$$\sigma_{yy} = B_1 \frac{\partial u}{\partial x} + B_2 \frac{\partial v}{\partial y} - B_3\theta, \tag{14}$$

$$\sigma_{xy} = B_4\left(\frac{\partial u}{\partial y} + \frac{\partial v}{\partial x}\right), \tag{15}$$

$$\frac{\partial^2 u}{\partial t^2} = \frac{\partial^2 u}{\partial x^2} + B_5 \frac{\partial^2 v}{\partial x \partial y} + B_4 \frac{\partial^2 u}{\partial y^2} - \frac{\partial \theta}{\partial x}, \tag{16}$$

$$\frac{\partial^2 v}{\partial t^2} = B_4 \frac{\partial^2 v}{\partial x^2} + B_5 \frac{\partial^2 u}{\partial x \partial y} + B_2 \frac{\partial^2 v}{\partial y^2} - B_3 \frac{\partial \theta}{\partial y}, \tag{17}$$

$$\left(\frac{\partial^2 \theta}{\partial x^2} + B_6 \frac{\partial^2 \theta}{\partial y^2}\right) = \left(1 + \tau_0 \frac{\partial}{\partial t}\right)\left(\dot{\theta} + B_7 \frac{\partial \dot{u}}{\partial x} + B_8 \frac{\partial \dot{v}}{\partial y}\right), \tag{18}$$

where

$$\left(B_1, B_2, B_4, B_5\right) = \frac{1}{A_{11}}\left(A_{12}, A_{13}, \mu_L, A_{21}\right),\ B_3 = \frac{\beta_{22}}{\beta_{11}},\ B_6 = \frac{K_{22}}{K_{11}},\ B_7 = \frac{T_0\beta_{11}^2}{\rho c_0^2 K_{11}\eta_0},$$

$$B_8 = \frac{T_0\beta_{11}\beta_{22}}{\rho c_0^2 K_{11}\eta_0}.$$

4 SOLUTION OF THE PROBLEM

For the analytic solution of eqs. (16)-(18) in the form of the harmonic travelling waves, we suppose the solution of the form:

$$\left[u, v, \theta\right]\left(x, y, t\right) = \left[u_1, v_1, \theta_1\right]\exp\left[\iota k\left(-x\cos\theta + y\sin\theta\right) - \iota\omega t\right], \tag{19}$$

where k is the wave number, ω is angular frequency having the definition $\omega = kV$, V being the phase velocity and $\left(\sin\theta, \cos\theta\right)$ denotes the projection of wave normal onto the *xy*-plane.

Substitution of (19) into eqs. (16)-(18) gives us

$$\left(C_{11}k^2 - C_{12}\right)u_1 - C_{13}k^2 v_1 - kC_{14}\theta_1 = 0\,, \tag{20}$$

$$C_{13}k^2 u_1 - \left(C_{21}k^2 - C_{12}\right)v_1 - kC_{22}\theta_1 = 0\,, \tag{21}$$

$$C_{31}ku_1 - C_{32}kv_1 + \left(C_{33}k^2 - \varepsilon\right)\theta_1 = 0\,, \tag{22}$$

where

$$C_{11} = \cos^2\theta + B_4\sin^2\theta\,,\ C_{12} = \omega^2\,,\ C_{13} = B_5\cos\theta\sin\theta\,,$$

$$C_{14} = \iota\cos\theta\,,\ C_{21} = B_4\cos^2\theta + B_2\sin^2\theta\,,\ C_{22} = \iota B_3\sin\theta\,,$$

$$C_{31} = \iota\varepsilon B_7\cos\theta\,,\ C_{32} = \iota\varepsilon B_8\sin\theta\,,\ C_{33} = \left(\cos^2\theta + B_6\sin^2\theta\right),$$

$$\varepsilon = \iota\omega + \tau_0\omega^2\,.$$

The condition for existence of non-trivial solution of system of above three equations provide us

$$V^6 + AV^4 + BV^2 + C = 0 \tag{23}$$

where

$$A = \frac{\left(D_{11}D_{25} - D_{24}D_{12} + D_{13}D_{22} - D_{14}D_{21}\right)\omega^2}{D},\ B = \frac{\left(D_{13}D_{23} - D_{12}D_{25} - D_{14}D_{22}\right)\omega^4}{D}$$

,

$$C = \frac{-\left(D_{14}D_{23}\right)\omega^6}{D},\ D = \left(D_{11}D_{24} + D_{13}D_{21}\right),\ D_{11} = C_{11}C_{22} - C_{14}C_{13}\,,\ D_{12} = C_{12}C_{22}\,,$$

$$D_{13} = C_{14}C_{21} - C_{22}C_{13}\,,\ D_{14} = C_{12}C_{14}\,,\ D_{21} = C_{11}C_{33}\,,\ D_{22} = C_{14}C_{31} - \varepsilon C_{11} - C_{12}C_{33}\,,$$

$$D_{23} = \varepsilon C_{12}\,,\ D_{24} = C_{13}C_{33}\,,\ D_{25} = C_{15}C_{32} - \varepsilon C_{13}\,.$$

The roots of equation (23) gives three values of V^2, which correspond to three coupled plane waves quasi-$P_1\left(qP_1\right)$, quasi-$P_2\left(qP_2\right)$ and quasi-$P_3\left(qP_3\right)$ propagating with velocities V_1, V_2 and V_3 respectively.

5 REFLECTION PHENOMENA AND BOUNDARY CONDITIONS

In this section, we shall investigate the reflection phenomena of a coupled plane wave $\left(qP_1\right)$ striking at the free boundary of considered half-space, propagating with velocity V_1 and making an angle θ_0 with the normal. In order to satisfy the boundary conditions, we postulate that this incident qP_1 wave gives rise to three reflected coupled plane waves qP_1, qP_2 and qP_3, making angles θ_1, θ_2 and θ_3 respectively with normal as shown in Fig. A. The full structure of the wave field consisting of the incident and reflected waves can be defined as:

$$(u, v, \theta) = (1, \eta_1, \zeta_1) A_0 P_0^- + \sum_{i=1}^{3} (1, \eta_i, \zeta_i) A_i P_i^+ , \tag{24}$$

where

$P_0^- = \exp\left[\iota k_1 \left(-x\cos\theta_0 + y\sin\theta_0\right) - \iota\omega_1 t\right]$ is the phase factor of the incident wave at angle θ_0 with A_0 as amplitude constant, $P_i^+ = \exp\left[\iota k_i \left(x\cos\theta_i + y\sin\theta_i\right) - \iota\omega_i t\right]$ are the phase factors of the reflected waves with amplitude constants

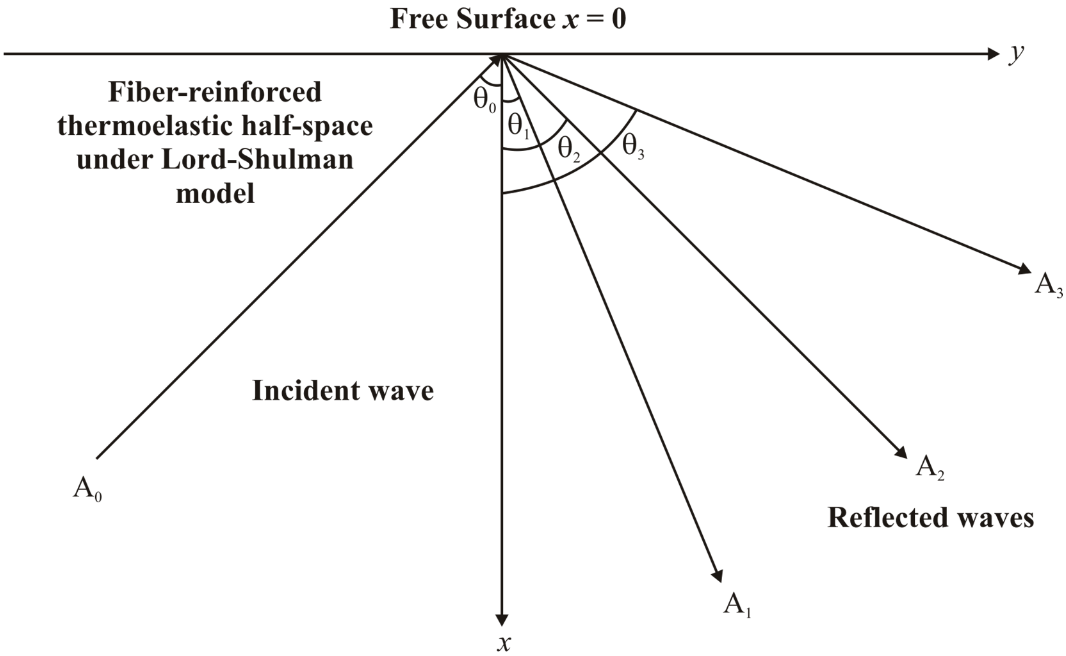

Fig. A: Geometry of the problem showing various reflected waves

A_i and η_i and $\zeta_i\,(i = 1, 2, 3)$ are the coupling parameters between u_1, v_1 and θ_1. The expressions of these coupling parameters are given by

$$\eta_i = -\frac{D_{11}k_i^2 - D_{12}}{D_{13}k_i^2 - D_{14}}, \quad \zeta_i = \frac{C_{11}k_i^2 - C_{12} - \eta_i\left(C_{13}k_i^2 - C_{14}\right)}{k_i C_{15}}$$

The amplitudes A_0, A_1, A_2 and A_3 can be determined from the boundary conditions at the free surface $x = 0$. Since, the boundary of the half-space is adjacent to vacuum, it is free from mechanical stresses. Therefore all components of stress tensor and the temperature must vanish at $x = 0$. Mathematically, these conditions may be expressed as:

$$\sigma_{xx} = \sigma_{xy} = \theta = 0 . \qquad (25)$$

The boundary conditions defined in equation (25) are identically satisfied if and only if $\omega = \omega_1 = \omega_2 = \omega_3$ and satisfy Snell's law, which gives the relation among angles of incident and reflected waves as:

$$k_1 \sin\theta_0 = k_1 \sin\theta_1 = k_2 \sin\theta_2 = k_3 \sin\theta_3 , \qquad (26)$$

which can also be expressed as (extended Snell's law):

$$\frac{\sin\theta_0}{V_1} = \frac{\sin\theta_1}{V_1} = \frac{\sin\theta_2}{V_2} = \frac{\sin\theta_3}{V_3} . \qquad (27)$$

Inserting the expressions of u, v and θ from equation (24) into expressions (13) and (15) and using relation given in (27), we obtain a system of three non-homogeneous equations in three unknowns by using the boundary conditions defined in (25). These three equations can be written in matrix form as:

$$\sum_{j=1}^{3} b_{ij} Z_j = Y_i, \quad i = 1, 2, 3 , \qquad (28)$$

where

$$b_{11} = k_1\left(\cos\theta_1 + B_1\eta_1 \sin\theta_1 - \frac{\zeta_1}{\imath k_1}\right),\ b_{12} = k_2\left(\cos\theta_2 + B_1\eta_2 \sin\theta_2 - \frac{\zeta_2}{\imath k_2}\right),$$

$$b_{13} = k_3\left(\cos\theta_3 + B_1\eta_3 \sin\theta_3 - \frac{\zeta_3}{\imath k_3}\right),\ b_{21} = k_1 B_4\left(\sin\theta_1 + \eta_1 \cos\theta_1\right),$$

$$b_{22} = k_2 B_4\left(\sin\theta_2 + \eta_2 \cos\theta_2\right),\ b_{23} = k_3 B_4\left(\sin\theta_3 + \eta_3 \cos\theta_3\right),$$

$$b_{31} = \zeta_1,\ b_{32} = \zeta_2,\ b_{33} = \zeta_3,\ Y_1 = -k_1\left(-\cos\theta_1 + B_1\eta_1 \sin\theta_1 - \frac{\zeta_1}{\imath k_1}\right),$$

$$Y_2 = -k_1 B_4\left(\sin\theta_1 - \eta_1 \cos\theta_1\right),\ Y_3 = -b_{31},\ Z_j = \frac{A_j}{A_0},\ \left(j = 1, 2, 3\right).$$

Here, $Z_j\left(j = 1, 2, 3\right)$ represent the reflection coefficients (ratio of the amplitudes of reflected waves to the amplitude of incident wave) of the reflected waves.

6 ENERGY PARTITION

In order to check the physical rightness of this problem, we must certify the energy balance during reflection at the free surface. Following Achenbach [20], the instantaneous rate of work of surface traction is the scalar product of the surface traction and the particle velocity. This scalar product is called the power per unit area, denoted by P^* and represents the rate at which the energy is transmitted per unit area of the surface. The time average of P^* over a period, denoted by $< P^* >$, represents the average energy transmission per unit surface area per unit time. For the present case, the rate of energy transmission at the free plane surface $x = 0$ is given by

$$P^* = \sigma_{xx}\dot{u} + \sigma_{xy}\dot{v}\,, \tag{29}$$

where superposed dot denotes temporal derivative. We shall now calculate P^* for the incident and each of the reflected waves using the appropriate potentials. The energy ratios $E_i\left(i=1,2,3\right)$ of the various reflected waves are defined as the ratios of energy corresponding to the reflected waves to the energy of the incident wave. The expressions for these energy ratios $E_i\left(i=1,2,3\right)$ for reflected waves are defined as:

$$E_i = \frac{< P_i^* >}{< P_0^* >}, \tag{30}$$

where $< P_0^* >$ denotes the average energy carried along incident wave and $< P_i^* >$ (i = 1, 2, 3) denote the average energy carried along reflected coupled waves. Thus, for an incident set of coupled wave having phase speed V_1, the energy ratios of reflected waves, by using expression (30), are given by

$$E_1 = P\left\{\cos\theta_1 + B_1\eta_1\sin\theta_1 - \frac{\zeta_1}{\imath k_1} + \eta_1 B_4\left(\sin\theta_1 + \eta_1\cos\theta_1\right)\right\} z_1^2\,,$$

$$E_2 = P\left\{\cos\theta_2 + B_1\eta_2\sin\theta_2 - \frac{\zeta_2}{\imath k_2} + \eta_2 B_4\left(\sin\theta_2 + \eta_2\cos\theta_2\right)\right\}\frac{k_2}{k_1} Z_2^2\,,$$

$$E_3 = P\left\{\cos\theta_3 + B_1\eta_3\sin\theta_3 - \frac{\zeta_3}{\imath k_3} + \eta_3 B_4\left(\sin\theta_3 + \eta_3\cos\theta_3\right)\right\}\frac{k_3}{k_1} Z_3^2\,,$$

$$P = \left\{-\cos\theta_1 + B_1\eta_1\sin\theta_1 - \frac{\zeta_1}{\imath k_1} + \eta_1 B_4\left(\sin\theta_1 - \eta_1\cos\theta_1\right)\right\}^{-1}, \tag{31}$$

where all the constants have been defined earlier.

7 PARTICULAR CASE

Neglecting fiber-reinforcement effect

In the absence of fiber-reinforcement, we shall be left with the relevant problem in a homogeneous thermoelastic medium in the context of L-S theory. In this case, it is sufficient to set the value of α, β and $\mu_L - \mu_T$ as $\alpha = 0, \beta = 0$ and $\mu_L = \mu_T$. Taking into consideration the above mentioned modifications, the corresponding reflection coefficients for the incidence of a set of coupled waves propagating with speed V_1 can be obtained from the system (28).

8 COMPUTATIONAL RESULTS AND DISCUSSION

In order to illustrate the contribution of fiber-reinforcement on the amplitude ratios, a numerical analysis is carried out. For the purpose of illustration, the material constants are taken from Abbas [11]:

$$\rho = 2660\, kg\, m^{-3},\ \lambda = 5.65\times10^{10}\ N/m^2,\ \mu_T = 2.46\times10^{10}\ N/m^2,$$

$$\mu_L = 5.66\times10^{10}\ N/m^2,\ \alpha = -1.28\times10^{10}\ N/m^2,\ \beta = 220.90\times10^{10}\ N/m^2,$$

$$K_{11} = 0.0921\times10^3\ Jm^{-1}s^{-1}\deg^{-1},\ K_{22} = 0.0963\times10^3\ Jm^{-1}s^{-1}\deg^{-1},$$

$$T_0 = 293\, K,\ \alpha_{11} = 0.017\times10^{-4}\deg^{-1},\ \alpha_{22} = 0.015\times10^{-4}\deg^{-1},$$

$$c_E = 0.787\times10^3\ Jkg^{-1}\deg^{-1},\ \tau_0 = 0.2\, s,\ \omega = 3.$$

With these numerical values of parameters, we have evaluated the amplitude ratios and energy ratios corresponding to incident qP_1 wave at different angles of incidence varying from normal incidence to grazing incidence. In Figs. (1-3), we have examined the variations of amplitude ratios in the considered medium for two different cases, (i) Fiber-reinforced thermoelastic medium under Lord-Shulman model (WRE, solid line) (ii) Thermoelastic medium under Lord-Shulman model (NRE, dashed line).

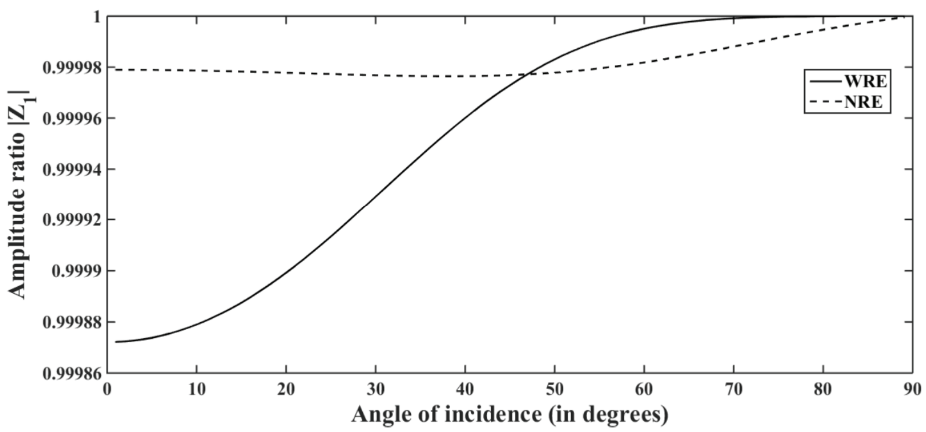

Figure 1: Effect of fiber-reinforcement on the moduli of reflection coefficient Z_1

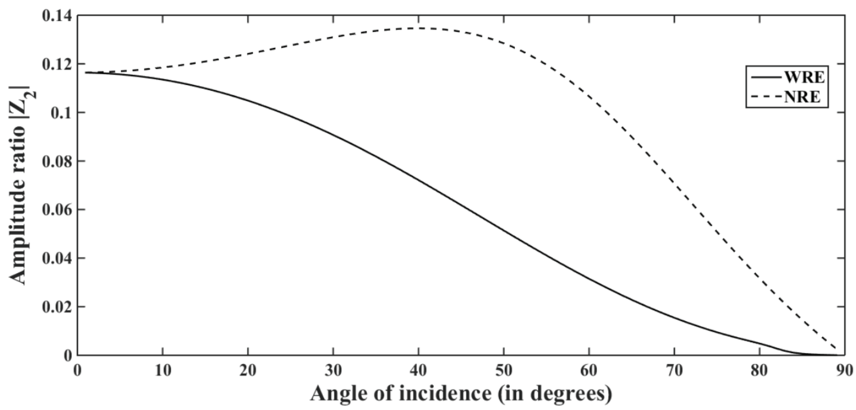

Figure 2: Effect of fiber-reinforcement on the moduli of reflection coefficient Z_2

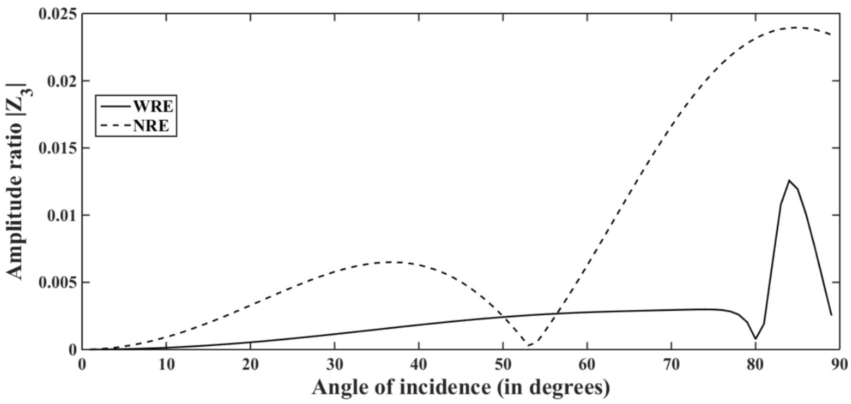

Figure 3: Effect of fiber-reinforcement on the moduli of reflection coefficient Z_3

In Fig. 1, we have illustrated the pattern of variation of reflection coefficient $|Z_1|$ versus angle of incidence in the presence and absence of fiber-reinforcement. It can be seen from the plot that the presence of reinforcement decreases the modulus values of Z_1 except in some range. Hence it has a mix effect on the profile of reflection coefficient $|Z_1|$. In Fig. 2, we have plotted the modulus values of the reflection coefficient Z_2 as a function of angle of incidence in the presence and absence of fiber-reinforcement. It can be noticed that the presence of fiber-reinforcement decreases the absolute values of reflection coefficient Z_2. So, it has decreasing effect on the profile of reflection coefficient $|Z_2|$ in whole range. The pattern of variation of reflection coefficient $|Z_3|$ against angle of incidence has been expressed in Fig. 3. For both cases (with and without fiber-reinforcement), it starts from zero value near normal incidence, thereafter increases and decreases with increase in angle of incidence in the whole range. It can be noticed that fiber-reinforcement has both increasing and decreasing effects on the profile of reflection coefficient $|Z_3|$.

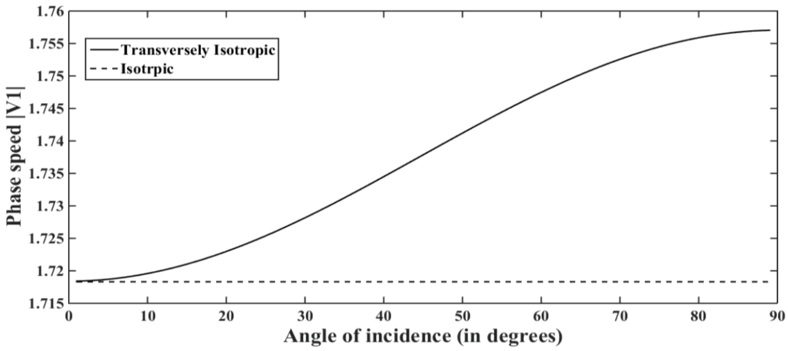

Figure 4: Variations of moduli of phase speed V_1 against angle of incidence to observe the effect of anisotropy

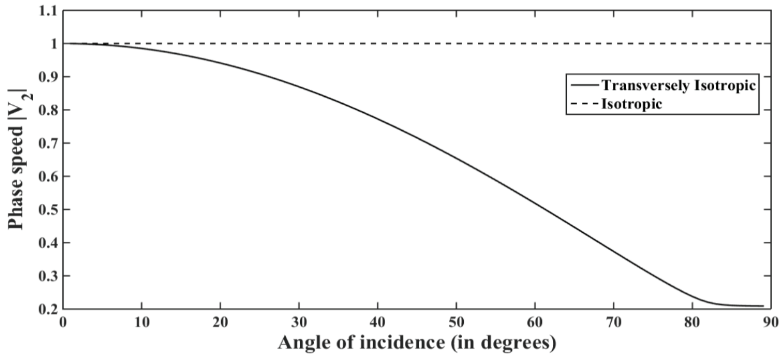

Figure 5: Variations of moduli of phase speed V_2 against angle of incidence to observe the effect of anisotropy

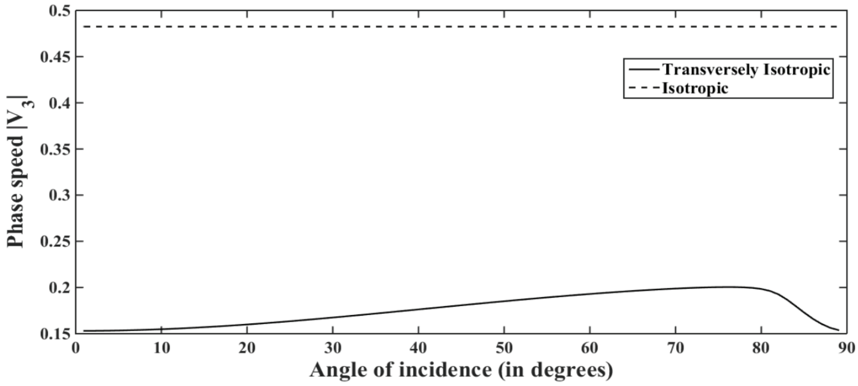

Figure 6: Variations of moduli of phase speed V_3 against angle of incidence to observe the effect of anisotropy

In Figs. (4-6), the variations in the velocities of qP_1, qP_2 and qP_3 waves have been shown graphically with the angle of propagation, when $\omega = 3$. The velocities of propagation of these plane waves are also compared with those for an isotropic thermoelastic media. We can see from these figures that the values of velocities vary at every angle of incidence in a transversely isotropic medium while in isotropic medium, these values remain constant throughout the whole range. Thus, it is evident from the figures that the medium has an observable effect on the variations of the velocities. It is noticed that there exist three waves propagating through the medium. It is also apparent from the Figs. (4-6) that the phase speed $|V_1|$ gets increased due to the presence of fiber-reinforcement (transversely isotropic medium). On the other hand, the phase speeds $|V_2|$ and $|V_3|$ attain smaller values in the presence of fiber-reinforcement. The fastest among them is the quasi-longitudinal wave and the slowest of them is the quasi-transverse wave.

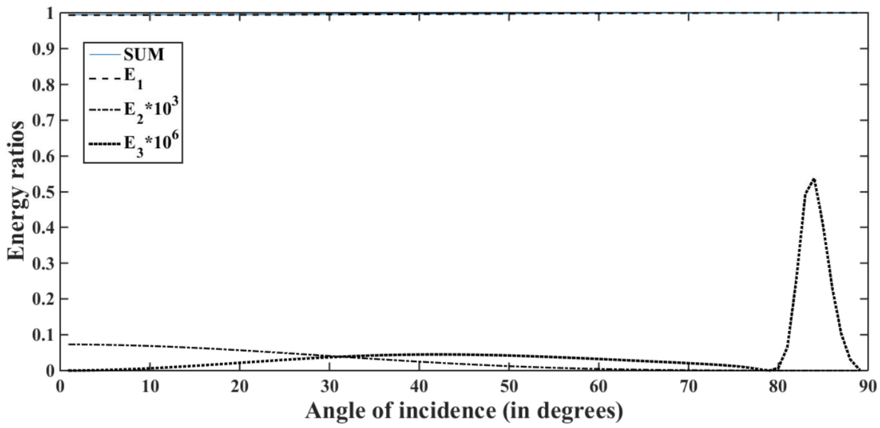

Figure 7: Variations of moduli of energy ratios

Fig. 7 reveals the variation of modulus of energy ratios of reflected waves with the angle of incidence of coupled wave propagating with velocity V_1. The energy conversion in different ranges of angle of incidence is clearly noticed. We can see from the figure that the values of sum and E_1 are approximately same and equal to 1.0, because the values of E_2 and E_3 are very small. Since the reflection coefficients Z_2 and Z_3 are found to be very small, therefore the corresponding energy ratios E_2 and E_3 are also very small. These energy ratios have been shown by dotted and dashed lines in figure after multiplying their original values by the factors 10^3 and 10^6 respectively. It can be seen from the figure that the energy carried by reflected coupled wave propagating with velocity V_1 is maximum in comparison to energy carried by other reflected waves. In the calculation of energy ratios, it has been verified that the sum of energy ratios is equal to unity. This shows that there is no loss of energy during reflection of waves.

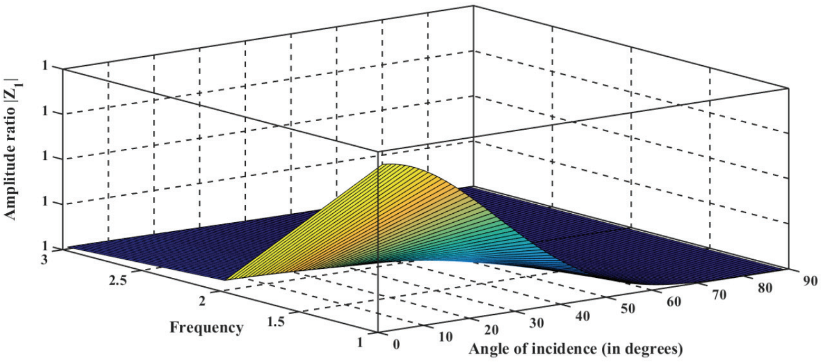

Figure 8: Profile of amplitude ratio |Z1| against angle of incidence and frequency

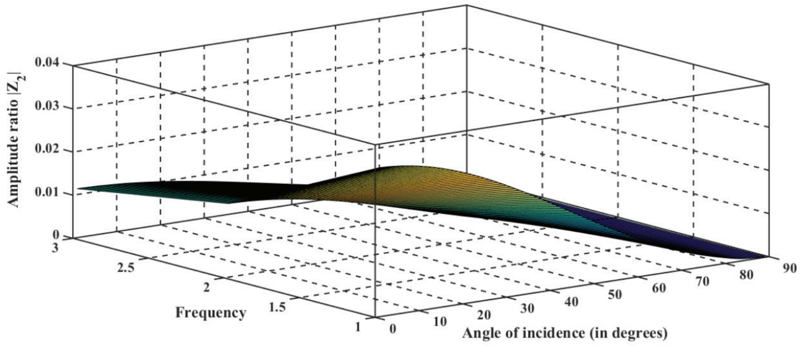

Figure 9: Profile of amplitude ratio |Z2| against angle of incidence and frequency

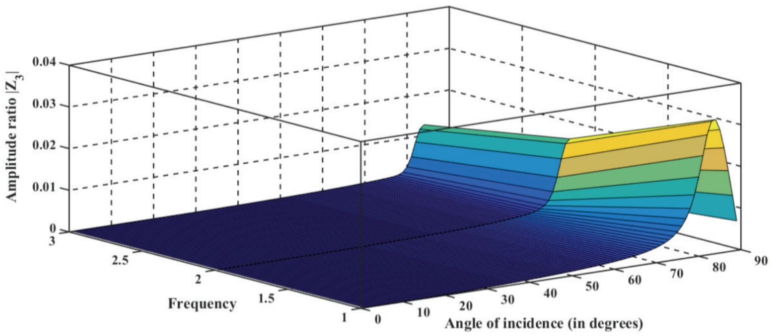

Figure 10: Profile of amplitude ratio |Z3| against angle of incidence and frequency

The 3D plots representing variations of amplitude ratios $|Z_1|, |Z_2|$ and $|Z_3|$ against angle of incidence θ and frequency ω, are shown in Figs. (8-10). Fig. 8 illustrates the variation of $|Z_1|$ with angle of incidence and frequency. From the figure, it is observed that the increase in the value of frequency results in decrease in numerical values of amplitude ratio Z_1. Modulus values of Z_1 increases with increasing angle of incidence. Fig. 9 indicates the variation of amplitude ratio $|Z_2|$ against angle of incidence θ and frequency ω. Numerical values of reflection that modulus values of Z_2 decreases with increasing frequency ω. It can be seen from the plot that modulus of values of Z_2 decreases as we increase angle of incidence. The variation of reflection coefficient $|Z_3|$ is plotted in Fig. 10 for wide range of θ and ω. Increment in the value of frequency has caused decrement in the numerical values of Z_3.

9 CONCLUSIONS

In this manuscript, a mathematical treatment has been presented to discuss the reflection phenomena in a fiber-reinforced thermoelastic medium under L-S theory. It has been observed that there exist three sets of coupled waves vibrating with distinct speeds. The effect of fiber-reinforcement is discussed numerically and illustrated graphically. The expressions giving the reflection coefficients and energy ratios have also been presented. From the analysis of the illustrations, we arrive at the following conclusions:

- The presence of fiber-reinforcement parameters decreases the absolute values of reflection coefficient Z_2 whereas on Z_1 and Z_3, its presence has both increasing and decreasing effects. Thus, all the reflection coefficients are significantly sensitive towards fiber-reinforcement.
- In an anisotropic generalized thermoelastic medium, the velocities of propagation of reflected waves are found to depend upon the angle of incidence, whereas in an isotropic medium, velocities attain constant values. Also, it is apparent from the figures that the phase speeds $|V_2|$ and $|V_3|$ get decreased due to anisotropy while the phase speed $|V_1|$ gets increased.
- Numerical results reveal that the sum of the modulus values of energy ratios at the free surface is approximately unity at each angle of incidence. This shows that there is no dissipation of energy during reflection phenomena at the free surface.
- The reflection coefficients and energy ratios depend upon the angle of incidence, the elastic properties of the half-space and the frequency of incident wave.

REFERENCES

[1] Lord H.W., Shulman Y., 1967, A generalized dynamical theory of thermoelasticity, *J. Mech. Phys. Solids.*, **15**:299-309.

[2] Green A.E., Lindsay K.A., 1972, Thermoelasticity, *J. Elast.*, **2**:1-7.

[3] Green A.E., Naghdi P.M., 1991, A re-examination of the basic postulate of thermomechanics, *Proc. Roy. Soc. London Ser. A.*, **432**:171-194.

[4] Green A.E., Naghdi P.M., 1992, On undamped heat waves in an elastic solid,

J. Therm. Stress., **15**:253-264.
[5] Green A.E., Naghdi P.M., 1993, Thermoelasticity without energy dissipation, *J. Elast.*, **31**:189-208.
[6] Belfield A.J., Rogers T.G., Spencer A.J.M., 1983, Stress in elastic plates reinforced by fiber lying in concentric circles, *J. Mech. Phys. Solids*, **31**:25-54.
[7] Chattopadhyay A., Choudhury S., 1990, Propagation, reflection and transmission of magnetoelastic shear waves in a self-reinforced medium, *Int. J. Eng. Sci.*, **28**:485-495.
[8] Sengupta P.R., Nath S., 2001, Surface waves in fiber-reinforced anisotropic elastic media, *Sadhana*, **26**:363-370.
[9] Singh B., Singh S.J., 2004, Reflection of planes waves at the free surface of a fiber-reinforced elastic half-space, *Sadhana*, **29**:249-257.
[10] Singh B., 2006, Wave propagation in thermally conducting linear fiber-reinforced composite materials, *Arch. Appl. Mech.*, **75**:513-520.
[11] Abbas I.A., 2011, A two-dimensional problem for a fiber-reinforced anisotropic thermoelastic half-space with energy dissipation, *Sadhana*, **36**:411-423.
[12] Gupta R., Gupta R., 2014, Reflection of waves in rotating transversely isotropic thermoelastic half-space under initial stress, *J. Solid Mech.*, **6**:229-239.
[13] Kumar R., Sharma K.D., Garg S.K., 2014, Effect of two temperatures on reflection coefficient in micropolar thermoelastic with and without energy dissipation media, *Adv. Acoust. Vib.*, **2014**:846721 (1-11).
[14] Kumar R., Ahuja S., Garg S.K., 2014, Surface wave propagation in a microstretch thermoelastic diffusion material under an inviscid liquid layer, *Adv. Acoust. Vib.*, **2014**:518384 (1-11).
[15] Ailawalia P., Sachdeva S.K., Pathania D., 2015, A two dimensional fiber-reinforced micropolar thermoelastic problem for a half-space subjected to mechanical force, *Theoret. Appl. Mech.*, **42**:11-25.
[16] Said S.M., Othman M.I.A., 2016, Gravitational effect on a fiber-reinforced thermoelastic medium with temperature-dependent properties for two different theories, *Iran. J. Sci. Tech. Trans. Mech. Eng.*, **40**:223-232.
[17] Abouelregal A.E., 2017, Fiber-reinforced generalized anisotropic thick plate with initial stress under the influence of fractional theory, *Adv. Appl. Math. Mech.*, **9**:722-741.
[18] Kalkal K.K., Sheokand S.K., Deswal S., 2019, Rotation and phase-lag effects in a micropolar thermo-viscoelastic half-space, *Iran. J. Sci. Technol. Trans. Mech. Eng.*, **43**:427-441.
[19] Deswal S., Sheokand S.K., Kalkal K.K., 2019, Thermo-diffusive interactions in a fiber-reinforced elastic medium with gravity and initial stress, *J. Brazilian Society Mechanical Sci. Eng.*, **41**:23-34.
[20] Achenbach, J.D., 1973, *Wave Propagation in Elastic Solids*, North-Holland, New York.